Iranian Journal of Medical Physics

ijmp.mums.ac.ir

Threshold of Linear and Non-Linear Behavior of High Intensity Focused Ultrasound (HIFU) in Skin, Fat, and Muscle Tissue Using Computer Simulation

Sare Mortazavi[1], Manijhe Mokhtari-Dizaji[1*]

1. Department of Medical Physics, Faculty of Medical Sciences, Tarbiat Modares University, Tehran, Iran

ARTICLE INFO

Article type:
Original Paper

Article history:
Received: Jul 19, 2021
Accepted: Nov 23, 2021

Keywords:
High Intensity Focused ultrasound
Non Linear
Pressure
Temperature
Distribution
Simulation

ABSTRACT

Introduction: In this study, the ultrasound-tissue interactions to obtain the resulting treatment thermal plans of high-intensity focused ultrasound (HIFU) are simulated.

Material and Methods: The simulations were performed for three layers of skin, fat, and muscle using Comsol software (version 5.3). The acoustic pressure field was calculated using the Westervelt equation and was coupled with Pennes thermal transfer equation to obtain thermal distribution. The pressure field was calculated and compared in two linear and non-linear models.

Results: By increasing the input sound intensity, the non-linear behavior becomes more pronounced and higher harmonics of the fundamental sound have appeared and increased the pressure, and temperature at the focal point. At input intensities of 1.5, 2, 5, 8, 10, 20, and 30 W/cm^2, the maximum acoustic pressure in the non-linear model compared to the linear model was 10, 11, 15, 22, 40, 47, 65, and 85%, respectively. The maximum temperature in the non-linear model increased by 9, 10, 12, 20, 22, 24, 31, and 45% compared to the linear model. Model results were validated with experimental results with a 95% correlation coefficient. The results of the input intensity 1.5, 2 and 5 W/cm^2 were acceptable ($p<0.05$) and from input sound intensity 8 W/cm^2 to above, there was a significant difference between the data ($p<0.05$). Also, maximum pressure and maximum temperature in the non-linear model are 20% more than in the linear model.

Conclusion: In the non-linear propagation model, the resulting thermal pattern changed significantly with the change of the input sound intensity.

► *Please cite this article as:*
Mortazavi S, Mokhtari-Dizaji M. Threshold of Linear and Non-Linear Behavior of High Intensity Focused Ultrasound (HIFU) in Skin, Fat, and Muscle Tissue Using Computer Simulation. Iran J Med Phys 2022; 19: 181-188. 10.22038/IJMP.2021.59077.1992.

Introduction

HIFU technology in medical treatment has grown significantly in recent decades. High-intensity focused ultrasound waves deliver their energy to the target tissue without damaging adjacent tissues [1]. The application of HIFU on skin tissue and at low penetration depths has grown significantly in the last two decades. HIFU was considered a non-invasive method for the skin, especially in the field of rejuvenation in the field of beauty. Using various treatment probs, heat induces at multiple depths, and causees the destruction of collagen, then new tissue is formed and collagen is regenerated, and finally, the skin is tightened and lifted [2]. Before reaching the target tissue, high-intensity focused ultrasound waves pass through the skin tissue, subcutaneous fat, and muscle. According to the tissue's viscosity coefficient, the acoustic pressure causes the tissue to move on the microscopic surface and convert to heat. An increase in temperature from 42-48 °C is called hyperthermia [3]. If the linear propagation of sound, the thermal rate depends on ultrasound waves intensity and tissue absorption coefficient. The absorption coefficient is dependent on frequency, and at higher frequency components, the non-linear factor enhances the thermal tissue rate [4].

High-intensity acoustic waves can change the parameters of the medium and destroy it. When a wave with high intensity propagates in the medium non-linearly, the waveform changes from the fundamental frequency to their harmonic frequencies that depend on the amplitude of the input sound intensity and the non-linear behavior of the medium and is defined by the non-linear parameter [5, 6]. The main advantage of HIFU is the local and point focus on the target. HIFU beam rapidly increases tissue temperatures. The focal area is typically oval in diameter, 1.5 cm long and 1.5 mm wide depending on the transducer frequency and focal geometry. Excitation conditions and geometrical shape of the transducer and sonication time, and its frequency can play a role in thermal distribution [7].

Treatment dependenceon sonication parameters and tissue type forces us to plan the treatment process using computer modeling [8]. Extensive studies have

*Corresponding Author: Tel: 98-21-82883893; Fax: 98-21-88006544; Email: mokhtarm@modares.ac.ir

been performed in simulating the propagation of ultrasonic waves and extracting the resulting thermal distribution assuming linear behavior [9]. Wave propagation is a non-linear phenomenon, especially in tissue. Linear equations, in conditions of high-pressure amplitude, are not a suitable solution to present a treatment plan [10, 11]. In several studies, the behavior of HIFU waves is linearly limited [12]. However, in other studies, the non-linear behavior of ultrasound propagation has been analyzed [13-15].

Today, studies on the linear propagation of ultrasound waves in the hyperthermia method have been considered, and treatment with HIFU waves and in the non-linear model is in its initial stages. Often the optimization of localization and control of therapy is related to cancer treatment. In these studies, the skin tissue and subcutaneous fat layer in the path of the waves were not examined. Due to the non-linear behavior of fatty tissue, in this study, based on the biophysical parameters of the skin layers and subcutaneous fat layer, the pressure map and the thermal scheme of the HIFU beam are simulated as the first passageway to enter the body. According to the non-linear behavior of subcutaneous fat, the pressure distribution map and thermal design of HIFU beam propagation with increasing sound intensity are simulated and compared in both linear and non-linear models. The intensity threshold will be extracted from the linear to a non-linear model.

Materials and Methods

The simulation was performed with Comsol (version 5.3) software using the finite element method (FEM) and solving pressure and temperature equations. In this study, the ultrasonic transducer is a spherical transducer with a curvature radius of 9 mm, an aperture radius of 5 mm, and a hole radius of 2.5 mm. The transducer frequency is 4 MHz, which is based on the treatment transducer of the doublo_s Hironic Korea devise. The geometry has axial symmetry. The cylindrical model geometry is 14×7 mm^2. The physical characteristics of layers (skin, fat, and muscle) are shown in Table 1. Between the probe and the skin is water (the acoustic impedance adaptation)

In a two-dimensional space, boundary conditions for solving the acoustic equation and the heat transfer equation were used. The acoustic pressure temporal rate is $P = P_0 \sin(\omega t)$. The radiation boundary on the walls without reflection is defined [11, 21]:

$$-\vec{n}.\left(-\frac{1}{\rho}\nabla p\right) = \frac{1}{Z_{mat}}\frac{\partial p}{\partial t} \quad (1)$$

Z_{mat} is the tissue acoustic impedance. $\vec{n}$ is a normal vector of a surface. $p = 0$ and $\frac{\partial p}{\partial t} = 0$ are initial conditions for acoustic propagation. Also, $T = T_0 = 310$ K is the initial condition for the heat transfer. To accurately calculate the propagation of a wave during medium, the mesh size must be small. If the transducer area is divided into more elements, the resolution was increased. In this study, the transducer surface was divided into parts with λ/6 size, and the focal zone into elements with λ/12 size (λ is wavelength). The time step in calculating the pressure distribution is of order 10^{-9} s. The solution time of the transient equation is of order 9×10^{-6} s. The solution time of the temperature distribution is of order 10^{-3} s. Different two-time scales are related to multi-physically numerical modeling [15, 22]. The acoustic wave takes about 1 μs to reach the region of interest (50-60 μs in this study). The model was simulated in the time-dependent domain. The pressure distribution maps in both axial and radial directions were extracted. In the linear model (β=0) and non-linear model (β ≠ 0), the Westervelt equation was solved and pressure distribution and temperature distribution were extracted, and compared in various intensities (1.5, 2.0, 5.0, 8.0, 10.0, 14.0, 20.0 and 30.0 W/cm^2).

The propagation of ultrasonic waves in the medium causes densities and expansions in the tissue [23]. Due to the effect of thermo-viscous, increasing pressure leads to an increase in temperature and the local velocity of sound in the medium. The high-pressure phase of the wave oscillates faster than the low-pressure phase. So the propagated waves that originally carried energy at the fundamental frequency of the source are now moving to higher harmonics. This distorts the waveform at the minimum and maximum, and the waveform leads to the sawtooth wave. The non-linear B/A parameter was calculated from the second-order expansion of the Taylor series of pressure in terms of density [24].

Table1. Input parameter of model

Parameter	water	skin	fat	muscle	reference
Speed of sound (m/s)	1430	1640	1450	1575	[16]
Density (kg/m^3)	1000	1100	911	1085	[17]
Non-linear coefficient	3.5	4.9	6.5	4.5	[17]
Attenuation coefficient at 4 MHz (dB/cm)	0.01	7.2	2.4	4	[14]
Thermal conductivity (W/m.K)	0.60	0.44	0.18	0.50	[18]
Heat capacity (J/kg.K)	4200	3300	2674	3768	[19]
Bulk viscosity (Pa.s)	0.024	0.024	0.04	0.024	[20]
Dynamic viscosity (Pa.s)	0.008	0.008	0.3	0.008	[17, 20]
Thickness (mm)	3.0	1.6	3.4	4	[18]

Non-linear effects lead to higher harmonics and consequently more attenuation and more heat transfer, especially in the focal region. The three most common equations for solving the non-linear behavior are the Burgers equation (1948), the Westervelt equation (1963), and the kzk equation (1970). The Westervelt equation is the general form of the non-linear wave equation, considering the diffraction, absorption, and thermo-viscous effects in all directions. The Westervelt non-linear equation assumes the absorption, diffraction, and thermo-viscous effects. The Westervelt equation does not have a known analytical solution, and because it is non-linear, the principle of overlap does not apply to it. Hence it was numerically calculated. Westervelt equation is solved by the finite element method. The acoustic pressure was obtained from the solution of the full-wave non-linear Westervelt equation [6, 11, 25]:

$$\nabla^2 p - \frac{1}{c^2}\frac{\partial^2 p}{\partial t^2} + \frac{\delta}{c^2}\frac{\partial}{\partial t}(\nabla^2 p) = -\frac{\beta}{\rho_0 c^4}\frac{\partial^2}{\partial t^2}(p^2) \quad (2)$$

The sound diffusivity (δ) is given by:

$$\delta = \frac{1}{\rho_0}\left(\frac{4}{3}\mu + \mu_B + \frac{(\gamma-1)k}{c_p}\right) \quad (3)$$

Where μ is the dynamic viscosity, μ_β is the bulk viscosity, γ is the heat capacity ratio, k is the thermal conductivity, and c_p is the specific heat capacity. The first two sentences show the Westervelt equation for linear behavior, the third sentence shows the loss due to heat conduction and the thermoviscous property of the fluid and the last sentence (right) refers to the non-linear behavior of a finite-amplitude wave [11, 22, 25].

In this study, the Westervelt full wave equation is used to solve the pressure field in non-linear propagation using Comsol software. The pressure distribution in adipose tissue as a target tissue was obtained. By solving the Westervelt equation and considering the thermo-viscous fluid, the equation was calculated in two states of linear (β = 0) and non-linear (β ≠ 0) pressure field. The equations were solved in the time-dependent domain. The Pennes heat transfer equation is used to calculate the temperature [11, 22,26, 27]:

$$\rho_t c_t \frac{\partial T_t}{\partial t} = k_t \nabla^2 T_t - w_b c_b (T - T_b) + Q \quad (4)$$

Indices t, and b, respectively, represent the parameters of tissue and blood. c, k, ρ, w and Q are the speed of sound propagation in the medium, the coefficient of thermal conductivity, density, the rate of blood perfusion, and the heat from the heat source, respectively. Here, the heat generated by the energy absorption of the HIFU sound wave in the tissue is obtained from Equations (5) and (6) [21, 22, 26, 27].

$$Q = 2\alpha_{avg} I \quad (5)$$

$$I = \frac{P_{rms}^2}{\rho c} \quad (6)$$

$$p_{rms}^2 = \frac{1}{t_f - t_i}\int_{t_i}^{t_f} p^2\, dt \quad (7)$$

t_i and t_f are the start and end times of the integration. The absorption coefficient is frequency dependent and is obtained from the following equation (25):

$$\alpha = \alpha_0 \left(\frac{f}{f_0}\right)^b \quad (8)$$

f_0 and α_0 are fundamental frequency and absorption coefficient. b for soft tissue is equal to1.

Results

The developed numerical method in the present work was validated in comparison with the solutions in the research literature based on the three-dimensional Westervelt equation and considering the effect of thermo-viscous and the average absorption coefficient for the tissue, with the results obtained from the experimental research [28]. Modeling was performed input parameter of the experimental study and the results of temperature distribution according to the depth of the present study were examined by a study [28] with Pearson correlation analysis and estimated with a confidence level of more than 95% ($p<0.05$). As shown in Figure 1, temperature data in terms of depth a focal area (z=8.5 cm) were compared with each other for the present study and the study [28]. (4 MHz frequency, 8.5 cm focal length, and 21 W input power).

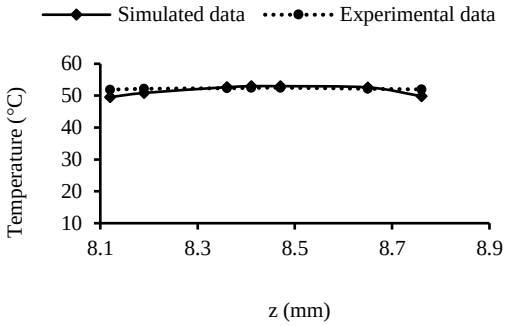

Figure 1. Comparison of temperature changes in both simulation and experimental study.

To compare and evaluate the linear and non-linear behavior of the Westervelt equation (Eq. 1) in two non-linear model (β ≠ 0) and linear model (β=0), for eight input intensities of 1.5, 2.0, 5.0, 8.0, 10.0, 14.0, 20.0, 30.0 W/cm^2 was calculated. These intensities are such as input transducer displacement amplitude (d_0) of 5.0, 6.2, 8.5, 11.3, 14.2, 16.2, 20.0 and 30.0 ηm. In the case of solving the non-linear equation, due to the production of higher sound harmonics as well as the non-linear parameter, a higher maximum pressure was observed.

To better understand the non-linear behavior of the pressure diagram for 5 input intensities of 1.5, 5.0, 8.0, 14.0, 20.0 W/cm^2 and in the radial direction at the focal point (z=8.6 mm) is given in Figure 2. As shown in Figure 2, increasing the intensity of the input sound leads to an increase in the maximum pressure in the focal region and distortion of the waveform, especially at the negative peak. As mentioned in the physics section of the model, the low-pressure part of the wave travels at a slower speed than the high-pressure part of the wave, and the symmetrical shape of the initial wave is destroyed.

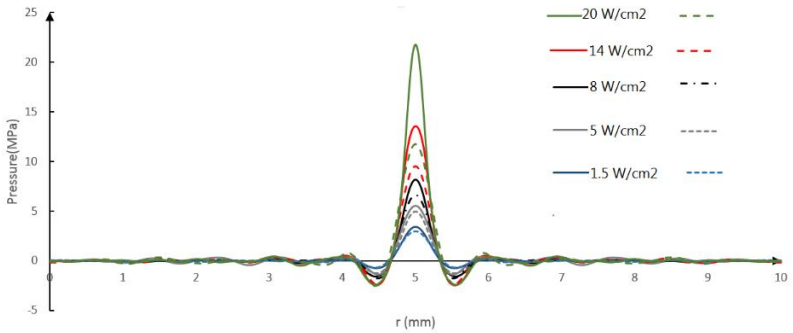

Figure 2. Radial pressure distribution diagram at the focal point of 8.6 mm for 1.5, 5.0, 8.0, 14.0, 20.0 W/cm^2 intensities in both linear (dotted) and non-linear (solid lines) models.

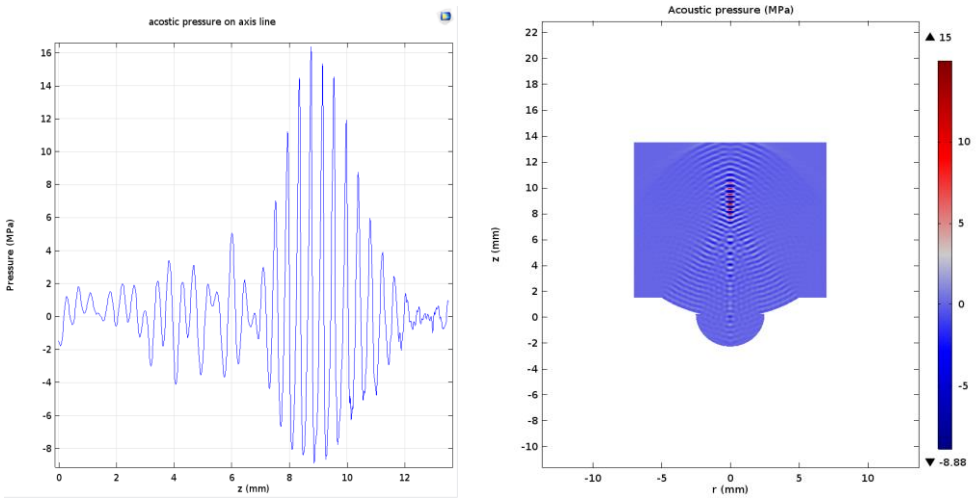

(a) (b)

Figure 3. Pressure distribution for 14 W/cm^2 intensity, a) in the longitudinal direction (z), b) pressure contour in the plate (z-r).

Table 2. Comparison of maximum and minimum acoustic pressure (MPa) in linear and non-linear model for 1.5, 2.0, 5.0, 8.0, 10.0, 14.0, 20.0, 30.0 W/cm^2 intensities.

Intensity (W/cm^2)	Maximum pressure p_+ (non-linear model)MPa	Minimum pressure p_- (non-linear model)MPa	Maximum pressure p_+ (linear model)MPa	Minimum pressure p_- (linear model)MPa	Percentage increase (%) $(p_{+nonlinear}-p_{+linear})/p_{+linear}$
1.5	3.33	-2.91	3.01	-3.03	10%
2	4.20	-3.49	3.78	-3.77	11%
5	5.52	-4.75	4.80	-4.70	15%
8	8.70	-6.09	7.11	-7.06	22%
10	12.00	-7.76	8.75	-7.86	40%
14	15.00	-8.80	10.20	-10.24	47%
20	20.30	-11.30	12.30	-12.20	65%
30	28.40	-18.30	15.30	-15.20	85%

Figure 2 shows the pressure distribution in the radial direction at the focal point for 5 input intensities in two models: linear (solid lines) and non-linear (dotted lines). With increasing the input sound intensity (8, 14, 20 W/cm^2). The difference between the solid line diagram and the dotted line of each intensity increases. This is due to the production of higher harmonics at the focal point at high input intensity. At low input intensity: 1.5 and 5.0 W/cm^2, the difference between linear and non-linear models is negligible.

Figure 3. Shows the longitudinal acoustic pressure distribution profile and pressure contour in the plate (z-r) MPa for 14 W/cm^2 input intensity.

The acoustic pressure distribution in the longitudinal direction (axis of central symmetry) is plotted in Figure 3a. The skin layer is z=4.5-6.1 mm, the fat layer is z=6.1-9.0.1mm and the muscle layer is z = 9.1 to14 mm. The amplitude of acoustic pressure reaches a maximum value in the focal area in the fat layer and after the transition from the focal area is damped in the muscle layer. Due to the focal nature of HIFU waves, the maximum pressure in the dimensions of 1.5×1.5 mm^2

occurs and energy is transferred to the adjacent tissues with minimal damage. In the linear model, for input intensity above (14 W/cm^2) the maximum positive and negative pressure is 10.2 MPa, which maintains its symmetrical waveform. Table 2 shows the maximum values of positive and negative pressure in both linear and non-linear models for input intensities of 1.5, 2.0, 5.0, 8.0, 10.0, 14.0, 20.0, 30.0 W/cm^2. Percentage increase of pressure was calculated based on maximum pressure at the non-linear model and linear model.

In the linear model, the wave is symmetrical, and there is no difference between the maximum and minimum pressure. Still, in the non-linear model with increasing input intensity, the wave becomes asymmetrical and distorted, and between the minimum and the maximum pressure, magnitude makes a difference. The percentage difference between the maximum positive pressure in both linear and non-linear models is given in Table 2. The frequency spectrum is plotted for 2 and 20 W/cm2 in linear and non-linear models (Figure 4). The vertical axis is the Fourier coefficient of pressure and the horizontal axis is frequency.

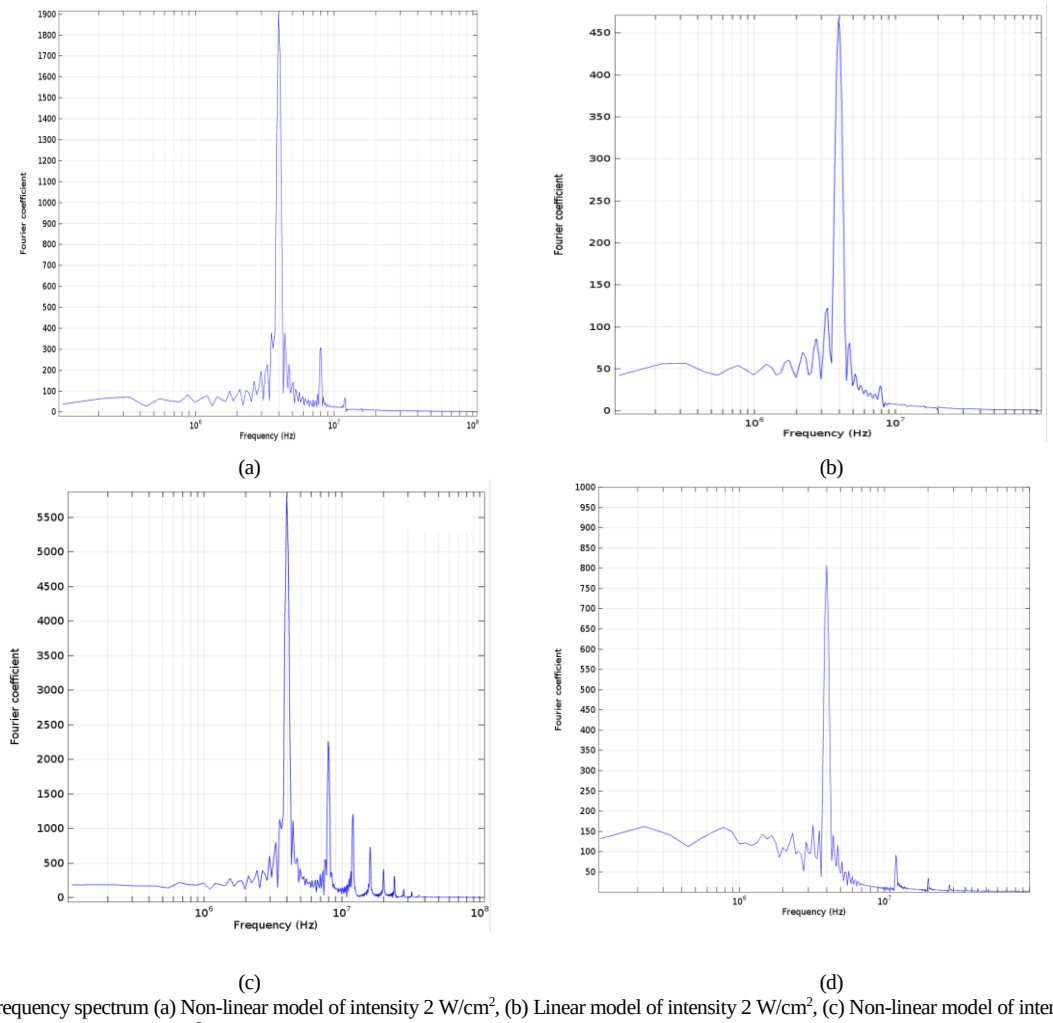

Figure 4. Frequency spectrum (a) Non-linear model of intensity 2 W/cm^2, (b) Linear model of intensity 2 W/cm^2, (c) Non-linear model of intensity20 W/cm^2, (d) Linear model intensity 20 W/cm^2

As the input intensity increases, the harmonic frequencies appear in the non-linear solution of the sound propagation (Figs. 4a and 4c), however the higher harmonics do not appear in the linear model (Figs. 4b and 4d). Also, increasing the input sound intensity, the number and amplitude of higher harmonics has increased (Figure 4d). This study's fundamental frequency or transducer frequency is 4 MHz, and the higher harmonic frequencies are 8, 12, 16, MHz (F = nf$_0$), respectively.

After calculating the pressure field and obtaining the rms (root mean square) pressure, and placing it in the heat transfer equations (Eq.3-6), the temperature distribution in the longitudinal and transverse directions was extracted for linear and non-linear models. Figure 5 shows the temperature distribution for 14W/cm^2 input intensity.

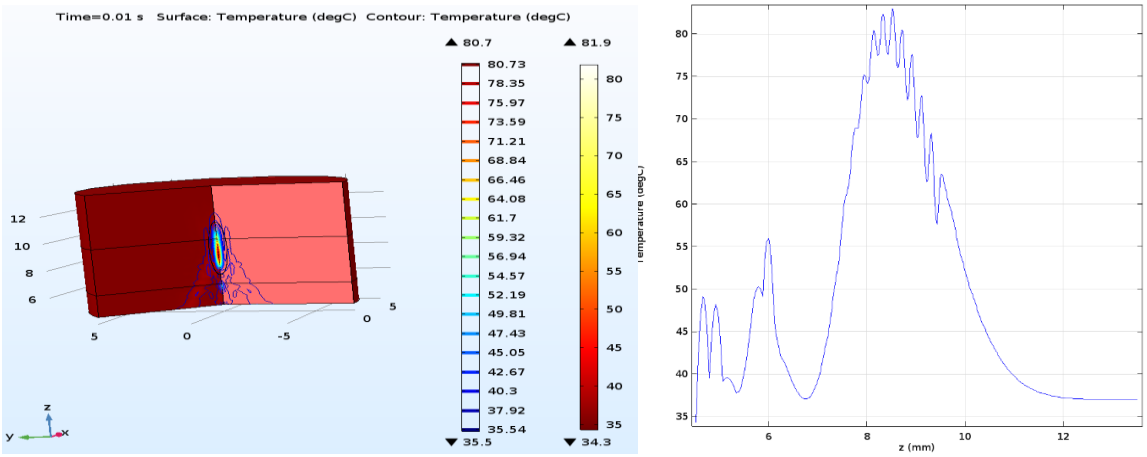

(a) (b)

Figure 5. a) Temperature contour on the plate (z-r), b) pressure distribution in the longitudinal direction (z)

In Figs. 5, the temperature contour and the temperature distribution are shown in (z-r) plate. First, due to the effects of thermo-viscous, small peaks appear on the skin layers (4.5 to 6 mm) and then in the focal area of the fat layer (7.5 to 9.5 mm). The maximum temperature is in 8.6 mm. After passing through the focal area in the muscle layer (9.5 to 14 mm), the ultrasound waves are attenuated.

The maximum temperature values in linear and non-linear model for the input intensities of 1.5, 2.0, 5.0, 8.0, 10.0, 14.0, 20.0, 30.0 W/cm^2 are given in Table 3.

Table 3. Comparison of maximum and minimum temperature in linear and non-linear models for 1.5, 2, 5, 8, 10, 14, 20, 30 W/cm^2 input intensities, *sonication time is=0.01 s*

Input intensity (W/cm^2)	Maximum temperature (non-linear model)°C	Maximum temperature (linear model)°C	Percentage increase (%) $(T_{+nonlinear}-T_{+linear})/T_{+linear}$
1.5	41	38	9%
2	44	40	10%
5	48	43	12%
8	70	58	20%
10	75	62	22%
14	81	65	24%
20	106	142	31%
30	146	212	45%

The percentage difference between the linear and non-linear models increases with the input sound intensity increases. To compare the temperature behavior at different intensities, the same sonication time is considered 0.01 seconds (10 ms). At high input intensities, the sonication time is reduced to the desired temperature of the device 60-70 °C. For example, the sonication time is 1 ms for 30 W/cm^2 intensity to reach the desired temperature of 60 °C.

The effect of input ultrasound intensity on the thermal plan, pressure, and temperature spectrum data versus depth for eight different input ultrasounds was statistically compared using ANOVA analysis by SPSS 16.0 software. Results showed except for the first three groups (1.5, 2.0 and 5.0 W/cm^2), the other groups (8.0, 10.0, 14.0, 20.0 and 30.0 W/cm^2) were significantly different ($p<0.05$). Thus, increasing intensity causes a significant change in the thermal plan in the fat layer.

Discussion

Other studies have used the Westervelt equation [11, 21, 25, 29] to solve non-linear sound propagation. In most studies, the target tissue is liver tissue and modeling for two layers of water and soft tissue is considered. The common frequency in most studies is 1 MHz at the depth of 10 cm. In the present study, the therapeutic transducer of the HIFU skin rejuvenation device with a low penetration depth (4.5 mm) in skin tissue and frequency of 4 MHz was modeled in three layers of skin, fat, and muscle. The focus of HIFU waves is located in the subcutaneous fat layer of the skin (considering the high non-linear coefficient of adipose tissue). The thermal-acoustic pattern of HIFU waves was calculated and extracted at the desired depth by adding the absorption and viscosity coefficients of skin, fat, and muscle. Due to the effect of frequency on the absorption coefficient, the average absorption coefficient for higher frequencies (up to the second frequency) was considered.

In limited studies, ultrasound propagation's linear and non-linear behavior has been compared [11, 29]. In paper [11], for input power 33.5, 75.4, and 134.0 W, the maximum pressure at the focal points 1.11, 2.50, and 4.00 MPa has been reported. The transition threshold from linear to non-linear behavior was expressed as 40 to 80 W. At 134 W input power, the maximum pressure in the non-linear model was two times higher than in the linear model. In this paper, the central frequency was 1 MHz, and the focal length was 50 cm. In this study, at the maximum input intensity of 30 W/cm^2, the maximum pressure ratioat the focal point in the non-linear model to 1.47 times the linear model is obtained.

As observed, considering the non-linear equations of ultrasound propagation and the effect of producing higher harmonics up to the second-order, at input intensities of 1.5, 5, 2, 8, 10, 20, and 30 W/cm^2, the maximum acoustic pressure in the non-linear model to

linear model 10, 11, 15, 22, 40, 47, 65 and 85%, respectively. The maximum temperature in non-linear models 9, 10, 12, 18, 21, 24, 31, and 45% relative to the linear model has increased. High intensities lead to a significant reduction in the time to reach the desired temperature for cell necrosis.. On the other hand, raising the pressure increases the cavitation phenomena [30], which making it difficult to control the clinical condition during treatment. Therefore, choosing the optimal intensity by considering all aspects according to the treatment goal and the desired temperature is essential. For selecting desirable intensity, it should be noted that the non-linear behavior increases with increasing the input sound intensity, and from the threshold intensity onwards, the emergence of non-linear behavior cannot be ignored. In this study, the intensity of the non-linear behavior threshold of 8 W/cm^2 was expressed. By ANOVA test using SPSS 16.0 software for intensities less than 8 w/cm^2, no significant difference was observed between the pressure and temperature distribution, while for intensities above 8 w/cm^2, the pressure and temperature distribution is different between the linear and non-linear models ($p<0.05$). So that at the input intensity of 8 W/cm^2, the linear equations do not respond to the wave behavior, and the maximum temperature in the non-linear model is 20% higher than in the linear model. As the input intensity increases, the heat generated in the focal region increases but the length of the focal region does not change.

Conclusion

The development of numerical calculations is essential for improving and developing the treatment plan for the use of ultrasound in therapeutic applications.In the present study, the design of acoustic and thermal pressure resulting from HIFU with emphasis on non-linear propagation of ultrasonic waves was extracted using computer modeling. The pressure field was calculated in both linear and non-linear models by solving the Westervelt equation and considering the thermo-viscous effect of the tissue. The symmetrical shape of the wave is degraded in the non-linear state relative to the linear state, especially in the focal zone. Increasing the maximum positive pressure relative to the maximum negative pressure removes the wave from the balanced state. The higher intensity, the more non-linear behavior and the more asymmetric the waveform appeared. In the non-linear model, higher harmonic frequencies than in the linear model are evident. The results showed at the threshold input intensity (8 W/cm^2), the pressure maps resulting from the non-linear model are not the same as the linear model. The maximum pressure in the non-linear model was higher than in the linear model ($p<0.05$). In the non-linear propagation model, with the change of the input intensity, the resulting sound pressure pattern changed significantly ($p<0.05$).

Acknowledgment

This study was approved by the Faculty of Medical Sciences, Tarbiat Modares University. This work was supported in part by the Iran National Science Foundation (INSF).

References

1. Al-Bataineh O, Jenne J, Huber P. Clinical and future applications of high intensity focused ultrasound in cancer. Cancer Treat Rev 2012; 38(5): 346-353.
2. Park JH, Lim SD, Oh SH, Lee JH, Yeo UC. High-intensity focused ultrasound treatment for skin: ex vivo evaluation. Skin Res Technol 2017; 23(3): 384-391.
3. Clarke RL, Bush NL, ter Haar GR. The changes in acoustic attenuation due to in vitro heating. Eur J Ultrasound 2003; 29(1): 127-135.
4. Ter Haar G, Coussios C. High intensity focused ultrasound: Physical principles and devices. Int J Hyperther 2007; 23: 89-104.
5. Wójcik J, Gambin B. Theoretical and numerical aspects of non-linear reflection–transmission phenomena in acoustics. Appl Math Model 2017; 46: 771-784.
6. Persson J, Hansen E, Lidgren L, McCarthy I. Modeling of the heat distribution in the intervertebral disk. Ultrasound Med Biol 2005; 31(5): 709-717.
7. Han H, Lee H, Kim K, Kim H. Effect of high intensity focused ultrasound (HIFU) in conjunction with a nanomedicines-microbubble complex for enhanced drug delivery. J Control Release 2017; 266: 75-86.
8. Martinez R, Vera A, Leija L. Finite element HIFU transducer acoustic field modeling evaluation with measurements. Pan Am Health Care Exchanges conference (PAHCE) 2012: 101-104.
9. Omena TP, Fontes-Pereira AJ, Costa RM, Simões RJ, von Krüger MA, de Albuquerque Pereira WC. Why we should care about soft tissue interfaces when applying ultrasonic diathermy: an experimental and computer simulation study. J Ther Ultrasound 2017; 5: 3-9.
10. Bailey MR, Khokhlova VA, Sapozhnikov OA, Kargl SG, Crum LA. Physical mechanisms of the therapeutic effect of ultrasound (a review). Acoust Phys 2003; 49(4): 369-388.
11. Haddadi S, Ahmadian MT. Analysis of nonlinear acoustic wave propagation in HIFU treatment using Westervelt equation. Scientia Iranica B 2018; 25(4): 2087-297.
12. Martínez R, Vera A, Leija L. HIFU induced heating modelling by using the finite element method. Phys Procedia 2015; 63: 127-133.
13. Guntur SR, Choi MJ. Influence of temperature-dependent thermal parameters on temperature elevation of tissue exposed to high-intensity focused ultrasound: numerical simulation. Ultrasound Med Biol 2015; 41(3): 806-813.
14. Grisey A, Heidmann M, Letort V, Lafitte P, Yon S. Influence of skin and subcutaneous tissue on high-intensity focused ultrasound beam: Experimental quantification and numerical modeling. Ultrasound Med Biol 2016; 42(10): 2457-2465.

15. Samanipour R, Maerefat M, Nejad HR. Numerical study of the effect of ultrasound frequency on temperature distribution in layered tissue. J Therm Biol 2013; 38(6): 287-293.
16. Van Sloun RJ, Pandharipande A, Mischi M, Demi L. Compressed sensing for beam formed ultrasound computed tomography. IEEE Trans Biomed Eng. 2015;62: 1-5.
17. Comley K, Fleck NA. A micromechanical model for the Young′s modulus of adipose tissue. Int J Solids Struct 2010; 47(21): 2982-2990.
18. Bhowmik A, Repaka R, Mishra SC. Thermal analysis of the increasing subcutaneous fat thickness within the human skin: A numerical study. Numer Heat Trans: A Appl. 2015; 67(3): 313-329.
19. Okabe T, Fujimura T, Okajima J, Aiba S, Maruyama S. Non-invasive measurement of effective thermal conductivity of human skin with a guard-heated thermistor probe. Int J Heat Mass Trans 2018; 126: 625-635.
20. Soneson JE, Myers MR. Thresholds for nonlinear effects in high-intensity focused ultrasound propagation and tissue heating. IEEE Trans Ultrason Ferroelectr Freq Control 2010; 57: 2450-2459.
21. Suomi V, Jaros J, Treeby B, Cleveland RO. Full modeling of high-intensity focused ultrasound and thermal heating in the kidney using realistic patient models. IEEE Trans Biomed Eng 2017; 65(5): 969-979.
22. Gupta P, Srivastava A. Numerical analysis of thermal response of tissues subjected to high intensity focused ultrasound. Int J Hyperther 2018; 35(1): 419-434.
23. Leighton TG. What is ultrasound? Prog Biophys Mol Biol 2007; 93: 3-83.
24. Hoffelner J, Kaltenbacher M. Finite element simulation of nonlinear wave propagation in thermoviscous fluids including dissipation. Trans Ultrason Ferroelectr Freq Control 2001; 48(3): 779-786.
25. Mohammadpour M, Firoozabadi B. Numerical study of the effect of vascular bed on heat transfer during high intensity focused ultrasound (HIFU) ablation of the liver tumor. J Therm Biol 2019; 86: 102431.
26. Namakshenas P, Mojra A. Microstructure-based non-Fourier heat transfer modeling of HIFU treatment for thyroid cancer. Comput Meth Prog Biol 2020; 197: 105698.
27. Abdolhosseinzadeh A, Mojra A, Hooman K. A porous medium approach to thermal analysis of focused ultrasound for treatment of thyroid nodules. Appl Acoust 2021; 182: 108236.
28. Kim J, Jung J, Kim M, Ha K, Lee E, Lee I. Distribution of temperature elevation caused by moving high-intensity focused ultrasound transducer. JPN J Appl Phys 2015; 54(7S1): 07HF13.
29. Gholami M, Haghparast A, Dehlaghi V. Numerical study for optimizing parameters of high-intensity focused ultrasound-induced thermal field during liver tumor ablation: HIFU Simulator. Iran J Med Phys 2017; 14(1): 15-22.
30. Ebrahiminia A, Mokhtari-Dizaji M, Toliyat T. Dual frequency cavitation event sensor with iodide dosimeter. Ultrason Sonochem 2016; 28: 276-282.